Received: 10 December 2021 | Revised: 7 June 2022 | Accepted: 8 June 2022 | Published on: 24 June 2022

DOI: 10.1002/joc.7763

RESEARCH ARTICLE

International Journal of Climatology RMetS

Winds are changing: An explanation for the warming of the Netherlands

Jippe Hoogeveen | **Han Hoogeveen**

Department of Information and Computing Sciences, Utrecht University, Utrecht, the Netherlands

Correspondence
Han Hoogeveen, Department of Information and Computing Sciences, Utrecht University, P.O. Box 80.089, 3508 TB Utrecht, the Netherlands.
Email: j.a.hoogeveen@uu.nl

Abstract

Western Europe is warming rapidly, much faster than the world average. To explain this phenomenon for the Netherlands, we look at the region where the airflow comes from instead of looking at the wind on the ground. Thereto, we consider 24 so-called weather patterns, which describe the origin of the airflow (north, northeast, etc.) and whether the airflow comes straight at us, or with bending of isobars (cyclonal or anticyclonal). For each day from January 1, 1836 onwards, we have determined the corresponding weather pattern on basis of the weather maps from Reanalysis archives at wettercentrale.de. Using a statistical test, we can see that a shift has occurred in the weather patterns, which has resulted in a significant increase in airflow coming from warmer directions. We further have applied linear regression to explain the daily average temperatures on basis of the weather patterns for the period 1961–2020. In this way, we find for the daily model an R^2 value of 0.60 and for the yearly model, based on the aggregated average daily values, we find an R^2 of 0.81, which is increased to 0.85 when we take the influence of the Atlantic Multidecadal Oscillation (AMO) and the Total Solar Irradiance (TSI) into account. These values strongly suggest that the warming in the Netherlands is caused by a shift in the origin of the airflow to warmer directions.

KEYWORDS

climate change, origin of the airflow, regression, the Netherlands, weather patterns

1 | INTRODUCTION

The Netherlands has warmed up very quickly in recent years, a lot faster than the world average (see, e.g., van Oldenborgh *et al.*, 2009). This warming has not taken place uniformly: there is a jump around 1988 of about one degree in the average temperature. We conjecture that this warming up and this jump in particular were caused by a change in the atmospheric circulation. To measure this, we need the temperature of the incoming airflow, for which we use as a proxy the *origin* of the airflow that comes to us. We have decided not to use the wind on the ground, which is for example used in Van Oldenborgh and Van Ulden (2003), since this is less accurate: it may occur that, for instance, airflow that originates from the SW region is registered as N wind on the ground. As there is no data available on the origin of the airflow, we have estimated manually for each day from

1836 until 2020 the atmospheric circulation on basis of the isobars in the weather maps from Wetterzentrale (see https://www.wetterzentrale.de/nl/reanalysis.php?model=noaa). In our classification we consider the 8 different geographic areas of origin, namely N, NE, E, SE, S, SW, W, and NW. Also, we estimate whether the airflow comes to us in a relatively straight line or with a bend. For the latter case, we have two different options: cyclonal and anticyclonal. This results in 24 different so-called *weather patterns* (WPs). Next to these, we allow the possibility of the score "A," which indicates that there is no airflow coming to us from far away; this mostly happens when there is an area of high or low pressure in the neighbourhood. We give a full description of the weather patterns in section 2. Our classification into the WPs is more extensive than the system used by Bergeron (1928), who identified air masses as Artic, Polar Maritime, Polar Maritime old, Polar Maritime warm, Polar continental, and Tropical. There is some resemblance to the classification system defined by Niedźwiedź in 1981 (see Niedźwiedź, 2006), but Niedźwiedź bases the classification on the direction at the end of the journey. The classification system by Lamb (1972) has a much stronger resemblance with our classification system, but there are some differences, which is why airflows with two totally different origins are classified as being of the same type.

We have used these WPs to perform several statistical experiments, which we describe in the remainder of this paper. First, in section 3 we compare our method with alternatives such as using the wind direction (on the ground) in De Bilt, the GrossWetterLage system (Gerstengarbe and Werner, 2005), the system by Niedźwiedź, and the system by Lamb. Next, in section 4 we compare the origins of the air masses in the periods 1961–1990 and 1991–2020 for each season to find out whether the circulation has significantly changed. In section 5 we look at the correlation between the average daily temperature and the wind patterns for the period 1961–2020. After stating our basic model, we present some adjustments to capture the influence of the sea. Next, we extend the model to the period 1836–2020, and we include the AMO (see https://en.wikipedia.org/wiki/Atlantic_multidecadal_oscillation), TSI (see https://en.wikipedia.org/wiki/Solar_irradiance) and CO_2. In section 6 we describe some experiments that we have applied to check the correctness of our model. Finally, in section 7, we draw our conclusions and suggest some directions for further research.

2 | CLASSIFICATION OF THE WEATHER PATTERNS

In a weather pattern we describe two components: the origin of the airflow, characterized by N, NE, E, SE, S, SW, W, NW, and whether it comes to us in a straight line or with a bend (G is no bend, C is a cyclonal bend and A is an anticyclonal bend). Since at some days there is not really a flow of air from somewhere far away, such days get the special type A. We have placed the boundary for "far away" at approximately 1,000 km. In Table 1 we indicate the regions by specifying an approximate centre and the two boundaries for the origins of the airflow.

In Figure 1, we specify six typical examples of WPs. The first four correspond to N, E, S, W without a bend in the flow. The latter two are examples of a cyclonal and an anticyclonal bend. Note that the example in (b) is on the boundary between E and NE. The weather maps come from Wetterzentrale. We have drawn a black path with an arrow in each picture to show the airflow to the Netherlands.

Next to the WPs, we have also manually estimated for each day the speed of the airflow and the pressure above the Netherlands. We estimated the speed on basis of the charts at the site of Wetterzentrale called "850 hPa stroomlijnen," where we simply divided the scale by 10 to get an integer from 0 to 7. For the air pressure above the Netherlands, which we can determine from the isobars, we use PH for values above 1,020 hPa, PL for values below 1,005 hPa and PT for the values in between. The only exception to this is when the WP is A: in that

TABLE 1 The eight origins of the airflow and their boundaries

Name	Centre	First bound	Second bound
N	Norway	Iceland	Finland
NE	NW-Russia	Finland	Belarus
E	Ukraine	Belarus	S-Romania
SE	Greece	S-Romania	E-Italy
S	East of Spain	E-Italy	Portugal
SW	Northeast of Azores	Portugal	North of Azores
W	Atlantic Ocean	North of Azores	S-Greenland
NW	Greenland	S-Greenland	Iceland

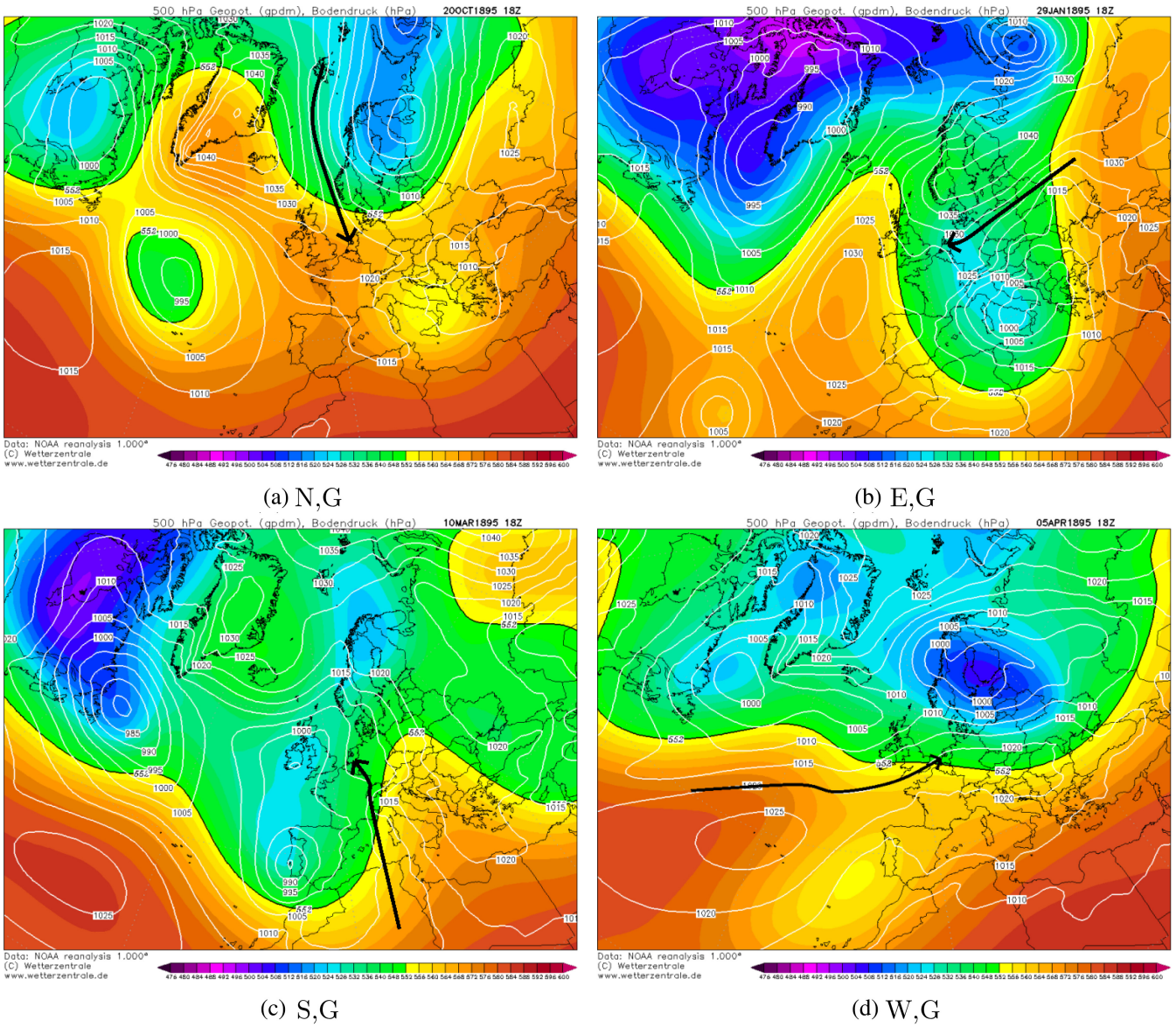

FIGURE 1 Examples of weather patterns. The first part indicates the origin; the second part the followed bend. The black arrow indicates the airflow to the Netherlands [Colour figure can be viewed at wileyonlinelibrary.com]

case there is almost always a pressure area above the Netherlands and hence we always use PH or PL.

This classification of the WPs is of course partially subjective. This is not a big problem as long as we make the same subjective choices over the entire period. To check this, we have performed a test in section 6: we have compared our WPs with the wind pattern on the ground from 1961 to 2020. In this way, we can check whether we have changed subjective choices over this period. We have made no attempt to specify criteria to come to an objectivization of our classification, like there exists for the GrossWetterLage system (see section 3), which has been objectivized by James (2007). We refer to Huth (1996) and Huth *et al.* (2008) for an overview on this topic.

The data can be downloaded from https://webspace.science.uu.nl/~hooge109/WP/Data.html.

3 | COMPARISON TO OTHER WIND CLASSIFICATION SYSTEMS

3.1 | Wind on the ground, KNMI

The KNMI (Koninklijk Nederlands Meteorologisch Instituut, i.e., the Royal Dutch Meteorological Institute), which is located in De Bilt, the Netherlands, has registered the wind on the ground from 1904 onwards. It is used by, for example, van Oldenborgh and van Ulden (2003) as a proxy for circulation type; van Oldenborgh

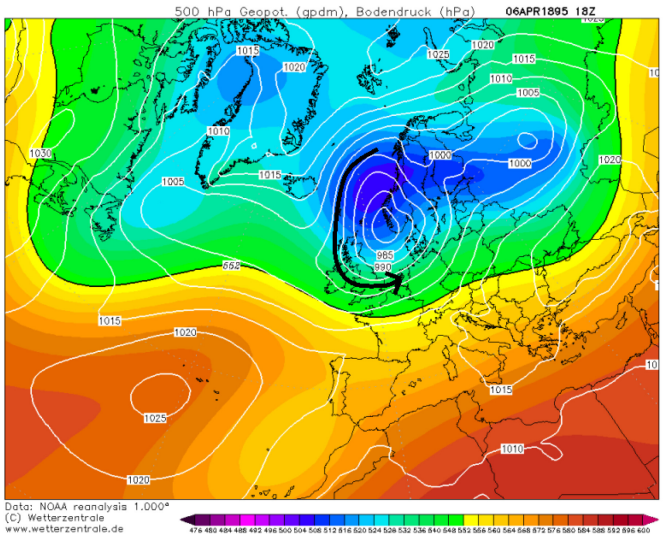

(e) N,C

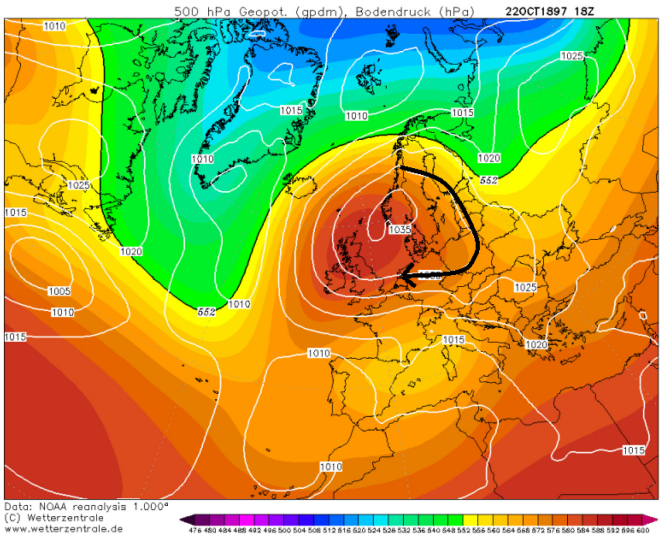

(f) N,A

FIGURE 1 (Continued)

TABLE 2 Difference percentage per sector between our weather patterns and the wind directions of the KNMI

Difference	Percentage	Cumulative (%)
0	20.1	20.1
1	38.7	58.8
2	25.0	83.8
3	13.2	97.0
4	3.0	100

TABLE 3 Difference percentage per sector between our direct weather patterns and the wind directions of the KNMI

Difference	Percentage	Cumulative (%)
0	23.7	23.7
1	43.0	66.7
2	22.2	88.8
3	9.0	97.8
4	2.2	100

and van Ulden state that "Locally measured wind direction gives the same results as geostrophic wind directions from pressure stations." Since the direction of the wind on the ground is determined by the last mile of the journey of the airflow towards us, this direction can easily deviate from the direction of the origin, which we use in our classification. Below we compute the similarity/difference between the two models. Since the measurements by the KNMI are specified in degrees, we first apply a preprocessing step by binning these to the eight sectors N, NE, until NW. If the degree falls in {23, 24, ..., 67}, then we consider the wind NE, and so on. Next, we simply compare for each day from 1904 to 2020 the sectors, where we exclude the days with the special type A. For each relevant day we compute the difference in sector (so N and NW differ exactly 1, while SE differs exactly 3 from W). Table 2 shows the results. Here *wind direction* corresponds to the binned direction of the wind on the ground.

In Table 2 we see that the wind direction differs often from the WP. For WPs with a bend it is likely that there is a difference, just because of the bend. To see if the two systems coincide in case of a WP without a bend (direct weather patterns, characterized with a "G"), we have repeated the experiment for the direct WPs only. This resulted in Table 3.

Even in case of direct WPs, the difference is quite large. Again, this is mainly because the wind direction only focuses at the last part of the airflow, but not on the entire airflow. Small bends at the end can therefore completely change the wind direction. Figure 2 shows examples of every difference. The first direction shows the direction according to the WP and the second direction shows the direction according to the wind direction. Once again we have drawn coloured paths with arrows to show the airflow; we have sometimes coloured the path red to enhance visibility.

The problem with wind direction is clearly demonstrated in these maps: small bends at the end of the airflow have way too much influence. The last example is a very unusual weather map, but examples (a) and (b) are quite common.

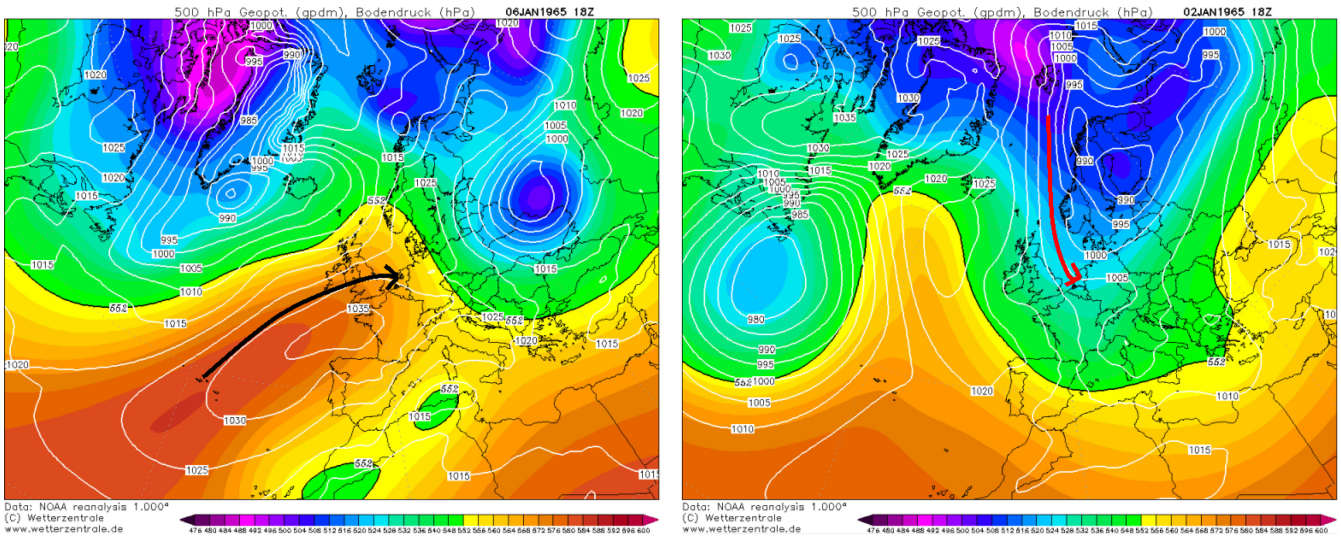

(a) SW, W (b) N, W

(c) N, SW (d) W, E

FIGURE 2 Examples of differences between weather patterns and wind direction. The first part indicates the origin according to our weather pattern; the second part the wind direction according to the KNMI [Colour figure can be viewed at wileyonlinelibrary.com]

3.2 | GrossWetterLage

The GrossWetterLage (GWL) is a system developed by German researchers and maintained by the Deutsche Wetter Dienst. The GWL is based on the situation in the whole of Europe. A description of the system (in German) can be found in Gerstengarbe and Werner (2005); this report contains the data for the period 1881–2004. Recent data can be found at the site of the Deutsche Wetter Dienst (see https://www.dwd.de/DE/leistungen/grosswetterlage/grosswetterlage.html). We do not have a full description of the GrossWetterLage system, but looking at the examples in the description it uses the pressure system to classify each day. A GWL must last for at least 3 days; otherwise, it falls in the category U ("unbestimmt," that is, unknown). There is no one-to-one correspondence between each GWL and the WPs. The main difference between the GWL and our WPs is that the GWL seems to look at the trajectory above Europe instead of the origin of the airflow. The Deutsche Wetter Dienst defines a code such as SWZ as an airflow from the southwest across Western and Central Europe, but this can correspond to winds from very different origins. Figure 3 shows 2 days with code SWZ with a very different origin of the airflow. Again, we have drawn coloured paths to show the airflow.

In the first example, the airflow comes from the sea between Portugal and the Azores to the Netherlands. In

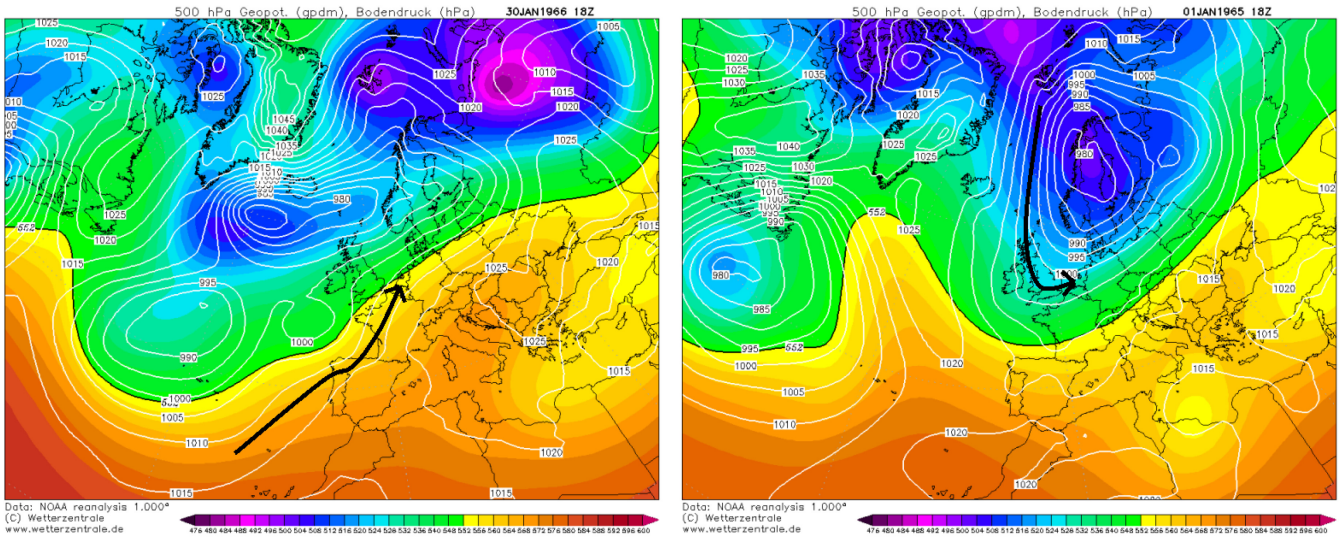

(a) Airflow from southwest (b) Airflow from north

FIGURE 3 Two examples of SWZ (southwest across Western and Central Europe) with very different origins of the airflows [Colour figure can be viewed at wileyonlinelibrary.com]

the second example, however, the airflow comes from the north across Great Britain to the Netherlands. Both examples have an airflow from the southwest above Western and Central Europe, but the main difference is that in the first example this airflow really starts southwest from the Netherlands, whereas in the second example, the airflow starts in the north and makes a sharp bend across Great Britain. This problem occurs in every classification system that focuses on the airflow above the Netherlands rather than the airflow to the Netherlands.

3.3 | Niedźwiedź's system

Niedźwiedź has presented a system to classify atmospheric circulations in 1981 (see Niedźwiedź, 2006), which is used to explain the temperature, precipitation, and air pollution concentration in Poland and Spitsbergen (Przybylak and Maszewski, 2009; Leśniok *et al*., 2010; Isaksen *et al*., 2016; Bartoszek and Matuszko, 2021). We do not have a description of the system of Niedźwiedź, but according to the examples in the papers that use it, Niedźwiedź's system also focuses on the airflow above the area of interest (in our study the Netherlands, but in theirs it is usually Poland). Hence, this system measures the direction of the wind at the end of the journey instead of where the airflow comes from.

3.4 | Lamb's system

Our classification system has the strongest resemblance to the classification system defined by Lamb (1972), which was used to specify the circulation patterns over the British Isles on a daily basis from 1861 to 1971. Lamb identifies seven different weather types: Anticyclonic, Cyclonic, Westerly, Northwesterly, Northerly, Easterly, and Southerly. According to the description of the system and the examples given in the paper, the circulation patterns are determined by the pressure systems. To determine the corresponding type Lamb checks the areas of high and low pressure. This resembles our classification, but we specifically look at the air flow, which can vary a bit within the same type depending on the exact position of the isobars. In Figure 4, we have placed some example of this. Both days have classification NW in the system of Lamb. This is because on both days, there is a high-pressure area at the southwest of the United Kingdom and a low-pressure area above Scandinavia. The main difference, however, is that in the first weather map, the high-pressure area does not extend far to the north whereas this is the case in the second weather map. This completely changes the flow from southwest to north. The arrows in Figure 4 indicate the flow towards the Netherlands. The difference with the United Kingdom is not very large.

4 | CHANGING FREQUENCIES OF WEATHER PATTERNS OVER TIME

In this section we look at how the observed weather patterns have changed over time. We have grouped them according to the origin of the airflow (so N,G; N,C; and N,A have been combined to N). For each year, for each season separately, we have counted the number of days

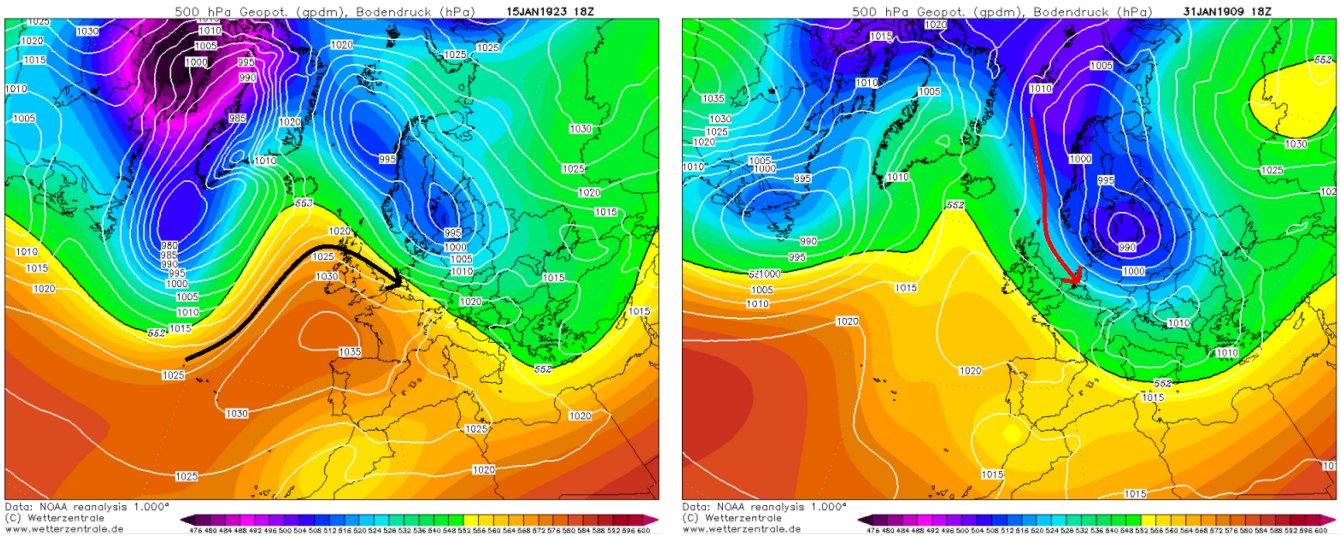

(a) Airflow from southwest (b) Airflow from north

FIGURE 4 Two examples of NW in Lamb's system with very different origins of the airflows [Colour figure can be viewed at wileyonlinelibrary.com]

with origin N, NE, until NW, respectively. These numbers are shown in Figure 5. Just to enhance clarity, we show SW, W, NW, N together as the group *Maritime* and NE, E, SE, S together as the group *Continental*. In the subfigures of Figure 5 we drew a continuous line through the loose points using a Loess curve with span 0.2. Remarkably there is an increase in the warm directions and a decrease in the cold directions in every season. In winter the frequencies of W and SW are nowadays extremely high while especially the frequencies of E, and NE to a lesser extent, have dropped. In spring the frequency of N has dropped extremely while SW, S, and SE have increased a bit. In summer N has dropped extremely and also NW is now very low. W has recently increased just as E, SE, S, and SW. In autumn N has again dropped extremely and SW and S have increased dramatically.

Based on these outcomes we have performed an independent two-sample t test to see if there is a significant change in each separate frequency between the periods 1961–1990 and 1991–2020 (see, e.g., the textbook by Walpole and Myers, 1993). This t test is defined as follows. Suppose for example that we want to test whether the frequency of N in the summer in 1961–1990 differs from the frequency of N in the summer in 1991–2020. We start by counting for each summer the number of days with N as area of origin. Given these values, we then calculate the average x_1 and standard deviation s_1 for 1961–1990; in a similar fashion we compute x_2 and s_2 for 1991–2020. Next we calculate the pooled sample variance,

$$s^2 = \frac{29 \cdot s_1^2 + 29 \cdot s_2^2}{58},$$

since in both 1961–1990 and 1991–2020 we have 30 data points. Now the t-statistic is calculated as

$$t = \frac{x_2 - x_1}{s \cdot \sqrt{\frac{1}{30} + \frac{1}{30}}}.$$

Since both groups consist of the same number of years, and since we may assume that both averages x_1 and x_2 are normally distributed because of the central limit theorem, we know that the t-statistic follows a t-distribution with 58 degrees of freedom under the null hypothesis that $x_1 = x_2$. We have also corrected for the leap days, but that has no big consequences. The results of this test are shown in Table 4. Periods I and II correspond to 1961–1990 and 1991–2020, respectively. Under the headers I and II we report the average number of days with an airflow from the given origin over the years in the respective period, for each season separately. These values do not add up to the number of days per season, because of the WPs with type A. The t-values (Table 4) are mentioned everywhere and the p-values (Table 4), are only mentioned if they are significant.

5 | INFLUENCE OF THE WEATHER PATTERNS ON THE TEMPERATURE

We have performed a regression to determine the effect of the atmospheric circulation on the temperature. In our computation we use all days from 1961 to 2020 as data

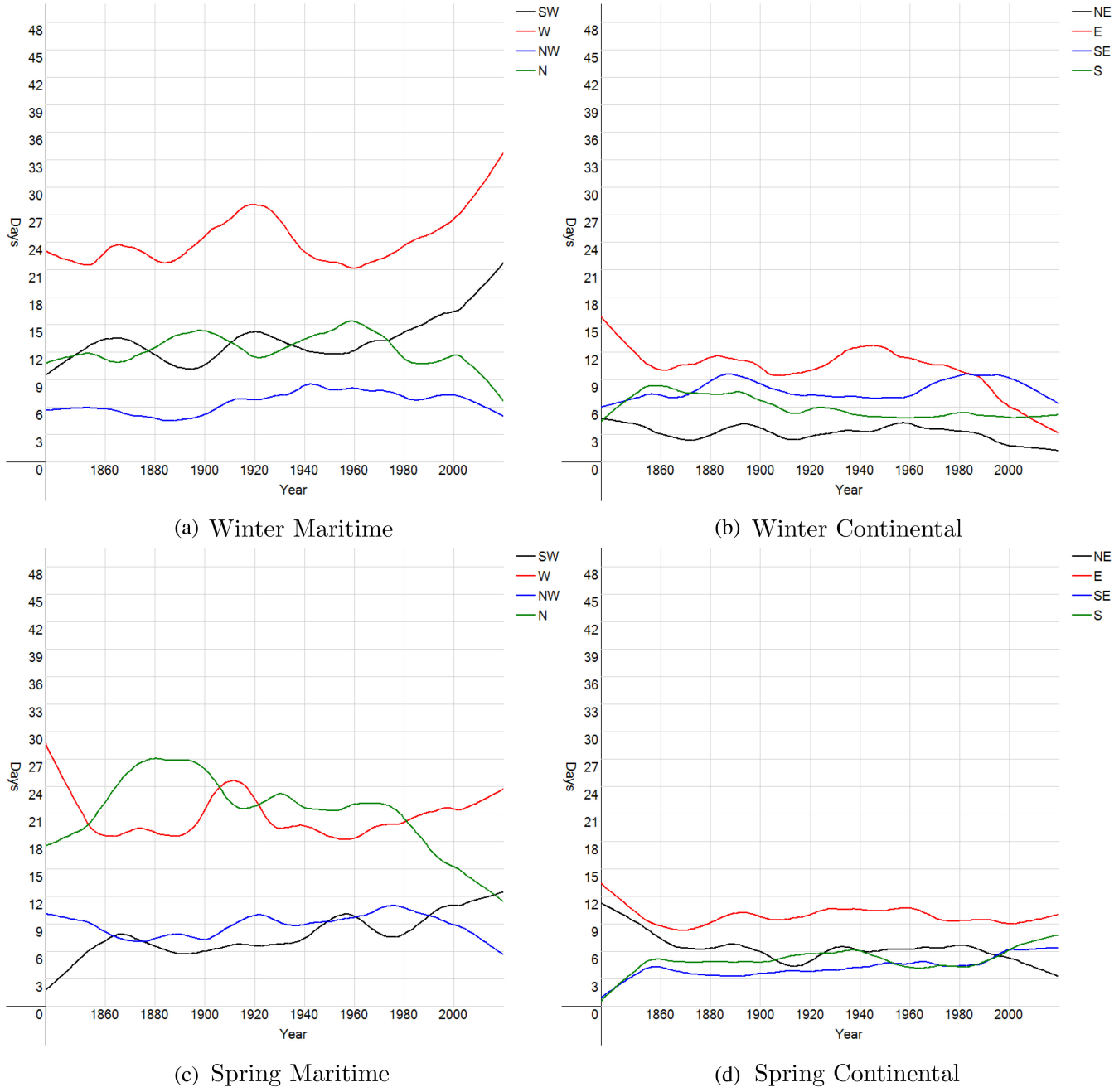

FIGURE 5 Changes in the observed weather patterns [Colour figure can be viewed at wileyonlinelibrary.com]

points. In a preprocessing step, we first compute the "normal temperature, normal amount of solar radiation, normal cloudiness, and normal wind speed" for each day in the year. Thereto, we use the data from the KNMI (see https://daggegevens.knmi.nl). These normal values are computed in the following way. Suppose that we want to compute the normal temperature. First of all, we calculate for each day (January 1–December 31) the average temperature on this day; in this way we get 366 averages. We then smooth these averages with an 11-daily moving average: the normal value for January 6 will become the average of the January 1's until the January 11's averages. This gives us a normal temperature on each day that is independent of the year; the computation of the normal values for solar radiation, cloudiness, and wind speed proceeds in the same fashion. Finally, we compute the normal amount of each weather pattern. Thereto, we first quantify the atmospheric circulation on each day, for each one of the 24 WPs; we thus sort of ignore the special type A. If a certain day has weather pattern N,G then we put the quantity N,G on this day equal to 1 and all the other 23 quantities are 0; for the other WPs we do the

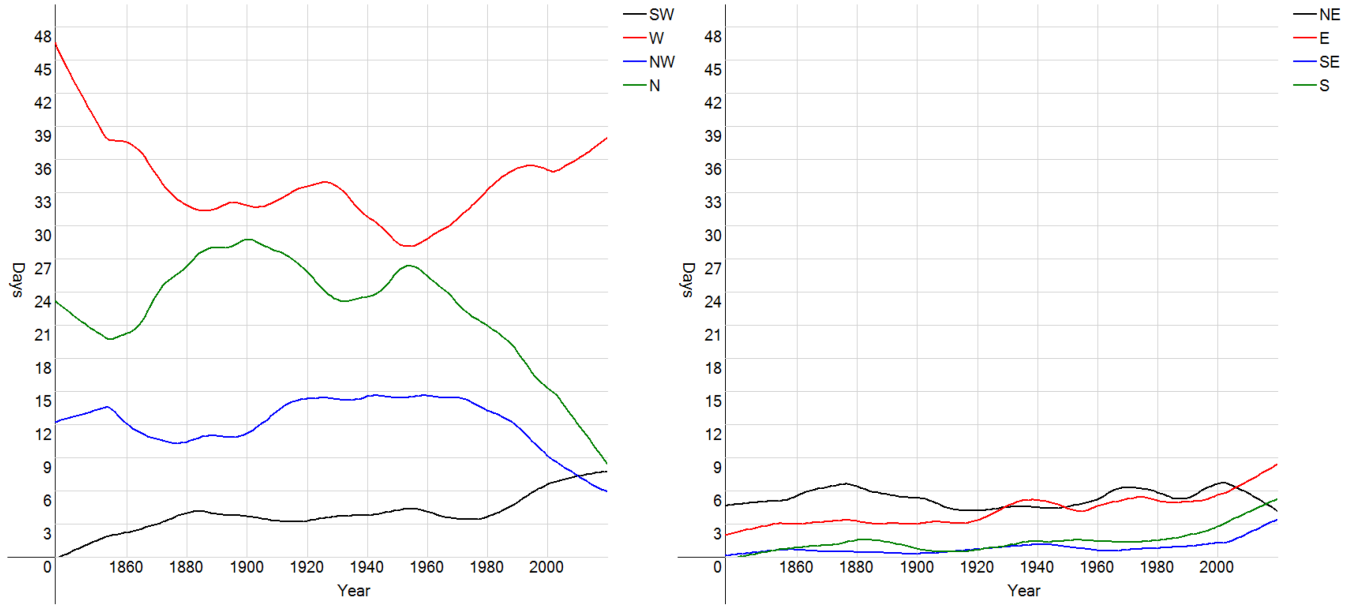

(e) Summer Maritime

(f) Summer Continental

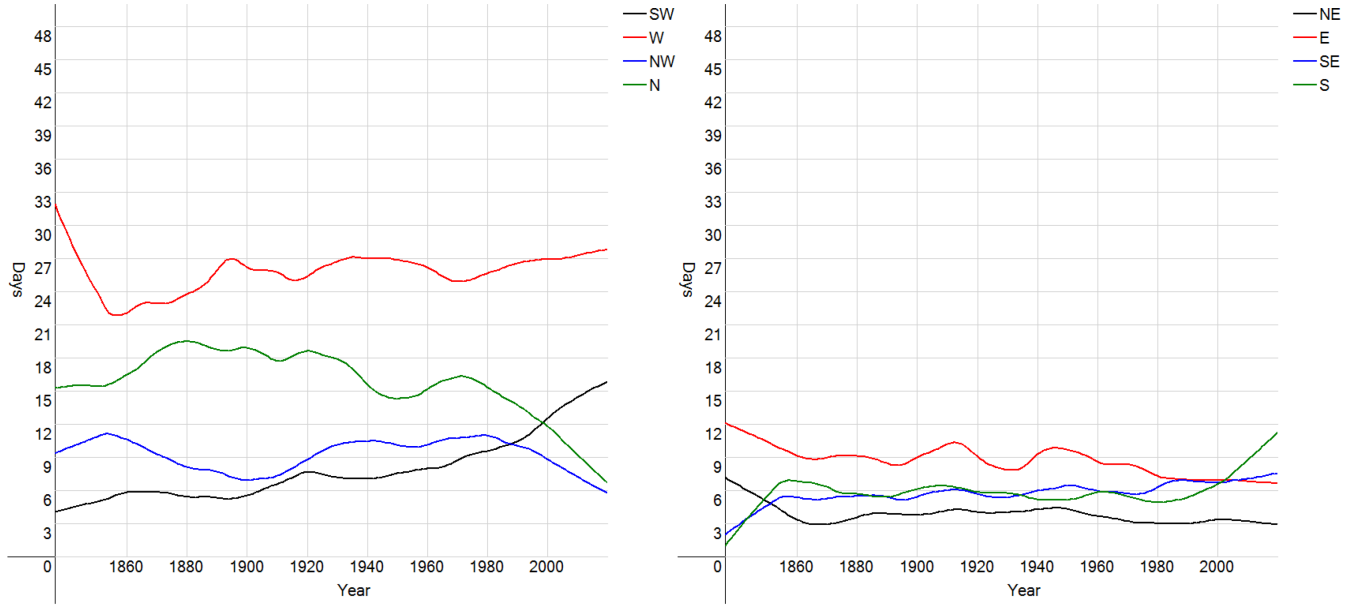

(g) Autumn Maritime

(h) Autumn Continental

FIGURE 5 (Continued)

same. If this day has weather pattern A, then every quantity of the 24 has value 0 on this day. We then calculate the normal amount of each weather pattern in the same way as we calculated the normal temperature.

Next we adjust each quantity (so the temperature, the solar radiation, the clouds, the wind speed and the 24 weather pattern quantities) by subtracting the corresponding normal on each day. In this way, we find the *anomalies*. In each of our regression models, we want to explain the temperature anomaly for each day. Hereto, we use explanatory variables based on the anomalies of the atmospheric circulation, solar radiation, cloudiness, and wind; in a consecutive step we add the influence of the sea. For the atmospheric circulation, we use for each weather pattern anomaly exactly four variables: one for winter, one for spring, one for summer and one for autumn. We use four variables per weather pattern to capture the influence of the seasons on the temperature changes caused by weather patterns; airflow from E, for instance, brings cold in winter and warmth in summer. Next, for each day in the year we calculate the so-called *season factor*. For January 16, the winter factor is 1 and

TABLE 4 Changes in weather patterns between the periods I (1961–1990) and II (1991–2020)

(a) Winter				
Origin	**I**	**II**	***t*-value**	***p*-value**
NE	3.7	1.6	−3.06	.003
E	10.3	5.6	−3.66	.0005
SE	8.9	8.6	−0.22	
S	4.9	5.0	0.08	
SW	13.7	17.2	2.09	.04
W	22.5	28.4	2.64	.01
NW	7.4	6.6	−0.92	
N	12.9	10.3	−1.76	
(b) Spring				
Origin	**I**	**II**	***t*-value**	***p*-value**
NE	5.9	4.8	−1.29	
E	9.5	9.1	−0.34	
SE	4.0	6.3	3.07	.003
S	4.4	6.6	2.73	.008
SW	8.0	11.4	3.38	.001
W	20.1	22.2	1.27	
NW	10.8	8.0	−3.23	.002
N	21.5	14.1	−4.02	.0002
(c) Summer				
Origin	**I**	**II**	***t*-value**	***p*-value**
NE	5.4	6.1	0.67	
E	4.9	6.4	1.73	
SE	0.7	1.8	2.7	.009
S	1.5	3.4	4.37	.00005
SW	3.4	7.0	5.05	.000004
W	32.4	35.9	1.88	
NW	13.9	8.3	−4.82	.00001
N	22.0	13.2	−5.07	.000004
(d) Autumn				
Origin	**I**	**II**	***t*-value**	***p*-value**
NE	2.8	3.2	0.62	
E	7.7	7.0	−0.88	
SE	6.0	7.0	1.18	
S	5.5	7.7	2.0	.05
SW	9.0	13.4	4.09	.0001
W	25.5	26.8	0.89	
NW	10.8	8.0	−2.7	.009
N	15.7	10.5	−3.77	.0004

all other factors have value 0; similarly April 16, July 16, and October 16 have value 1 for the spring factor, summer factor, and autumn factor, respectively (and value 0 for the other factors). Then the factors of the remaining days are computed by looking at which days of January 16, April 16, July 16, and October 16 are closest by, after which a weighted average is taken on basis of the distance in number of days. Take for example January 5, which is in between October 16 and January 16. Since January 16 is the 92nd day after October 16, the winter factor of January 5 is 81/92 and the autumn factor of January 5 is 11/92. For each weather pattern anomaly, we have a variable for winter, spring, summer and autumn. On a certain day we multiply the weather anomaly on that day with each corresponding season factor and we do the same for the 4 days before, after which we take the average over these 5 days. Take for example January 5, 1961; it has winter factor 81/92 and autumn factor 11/92. For January 1–4 we find winter factors 77/92 until 80/92 and autumn factors 15/92 until 12/92. To clarify the regression for this example, we introduce the following notation. Let β_1, ..., β_{24} denote the variables (which are to be estimated by the linear regression) for the 24 WPs for winter and let β_{73}, ..., β_{96} denote the ones for autumn. Furthermore, let us denote the anomalies of the 24 WPs for January k ($k = 1, 2, 3, 4, 5$) in 1961 by $q_{1,k}$, ..., $q_{24,k}$ as defined above. Then the part corresponding to the WPs in the linear regression model for January 5, 1961 becomes equal to

$$\left[\frac{81}{92}\sum_{j=1}^{24} q_{j,5}\beta_j + \frac{80}{92}\sum_{j=1}^{24} q_{j,4}\beta_j + \frac{79}{92}\sum_{j=1}^{24} q_{j,3}\beta_j + \frac{78}{92}\sum_{j=1}^{24} q_{j,2}\beta_j + \frac{77}{92}\sum_{j=1}^{24} q_{j,1}\beta_j + \frac{11}{92}\sum_{j=1}^{24} q_{j,5}\beta_{j+72} + \frac{12}{92}\sum_{j=1}^{24} q_{j,4}\beta_{j+72} + \frac{13}{92}\sum_{j=1}^{24} q_{j,3}\beta_{j+72} + \frac{14}{92}\sum_{j=1}^{24} q_{j,2}\beta_{j+72} + \frac{15}{92}\sum_{j=1}^{24} q_{j,1}\beta_{j+72}\right]/5.$$

We have chosen to use also the data of 4 days before because the air is not directly transported from the area of origin to the Netherlands. Together with the variables corresponding to solar radiation, cloudiness, and wind anomaly we now have 99 explanatory variables and we explain the temperature anomaly with them on all days of 1961–2020. Here we use the standard assumption that the errors are independent and normally distributed. Using this, we get an $R^2 = 0.60$ so we explain 60% of the

daily variance in temperature. We have a total of 21,915 data points and 99 explanatory variables, so there are exactly 21,915–100 = 21,815 degrees of freedom.

In a consecutive step, we take the effect of the sea into account, since it reacts slowly on changes in the temperature compared to the surface (see, e.g., van *Oldenbo*rgh et al., 2009). To simulate this, we use a very simple model in which the heat transfer from the air to the sea is proportional with the difference in temperature. This effectively means that the sea reacts with a certain factor f to changes in the air temperature. This means in our model that if the current sea temperature is t_1 and the air temperature is t_2, then the sea temperature tomorrow will be $(1-f)\cdot t_1+f\cdot t_2$. We have chosen $f = 0.035$. For this choice for f the sea water temperature in a month from now is determined for approximately 1/3 by the current sea temperature and for 2/3 by the air temperatures of the coming month. We now proceed as follows. We apply the first regression (as described above), and consider the estimated temperature anomaly as the anomaly of the *air temperature*. Next, we use these values to estimate the anomaly of the sea temperature, using $f = 0.035$. Then, we apply a second linear regression model, in which we try to explain the anomalies of the measured temperature on basis of the estimates of the air and sea temperature (hence, there are only two variables in this regression). We have chosen to use the estimated temperature instead of the measured temperature in our estimation of the sea temperature to eliminate all possible side-effects caused by other factors than the WPs, solar radiation, cloudiness, and wind.

We have also expanded this to the years 1836–1960: unfortunately, we do not have good data for the solar radiation, clouds or wind speed before 1961. We have tried to estimate these values on basis of the weather patterns. We do pretty much the same as with the temperature, except that we use the speed of the airflow as well: if a day has for example N,G as weather pattern and the speed of the airflow is 3, then we count 3 at the quantity N,G and 0 at the other weather quantities on this day. If on the other hand the speed of the airflow was 2, then we had counted 2 at N,G. We count 0 everywhere in the case of a WP with type A. We also use three additional quantities, namely whether there was PH, PT, or PL as pressure. At these, we only count 1 if it happened and 0 otherwise. We then apply a similar regression as we did to explain the temperature anomaly, but now we explain the solar radiation, clouds and wind speed. We use all days from 1961 to 2020 as data points and calculate for each of these days the anomalies. We use the season factors again, which means that we get for each weather anomaly four times as many variables and we do the same for the three pressure anomalies. In this way, we explain the solar radiation, clouds and wind speed in the period 1961–2020 on basis of the WPs, speed of the airflow, and pressure. Now, since we know for each day in the period 1836–1960 the WPs, speed of the airflow, and the pressure, we can use the values found in the regression to estimate the values for solar radiation, clouds, and wind speed for each day in the period 1836–1960. Finally, we use these estimates in our regression model to estimate the temperature of each year from 1836 to 2020 based on the weather patterns and the other factors. In Figure 6, we compare the temperatures estimated by the regression model to the real data, where we take the average temperature per year. In the second graph, we plot the residual using a Loess curve with span 0.2.

Unfortunately, the data before 1900 is not extremely reliable: we used the Labrijn-reeks (see https://www.wintergek.nl/data/lijst-gemiddelde-temperatuur-nederland) to calculate the mean temperature of each year, but it is less reliable than the temperature measurements from 1901 in De Bilt. Also, the older weather maps are less reliable. There is also something strange with the cloud data from 2016 until 2020: it is way higher than before and also higher than should be expected according to the weather patterns. This is most likely because the way of measuring the clouds has changed in 2016 and the KNMI has not yet corrected the data for this change. We therefore only use the data from 1901 to 2015. We get $R^2 = 0.81$ approximately for the *yearly average* temperature.

We also want to explain the residuals from 1901 to 2015. We do this again with regression and we use the following three variables: the TSI, the AMO, and the CO_2. Data for these variables can be found at the site of the KNMI (see https://climexp.knmi.nl/start.cgi). We used a 11-year moving regression for the TSI to filter out the influence of the 11-year sunspot cycle. For the CO_2, we use the total downward forcing caused by it (so doubling the CO_2-levels gives approximately 4 $W\cdot m^{-2}$ extra forcing). If we do this regression, we get that the factor for the TSI is 0.58 ± 0.30, the factor for the AMO is 0.54 ± 0.30 and the factor for the CO_2 is -0.01 ± 0.15 where the $\pm$ values give the 95% confidence interval. We have calculated these intervals based upon a t test for regression. To do this, we first needed to calculate for each year the difference between the regression based upon TSI, AMO, and CO_2 and the actual data (so the mean temperature of that year minus the temperature according to the weather patterns). We square all these differences and add them up; we denote this value with S. We also have 115 data points and three explanatory variables, so there are 115–4 = 111 degrees of freedom. Next, we calculate the covariance matrix of the TSI, AMO, CO_2, and the constant. We can find the variances

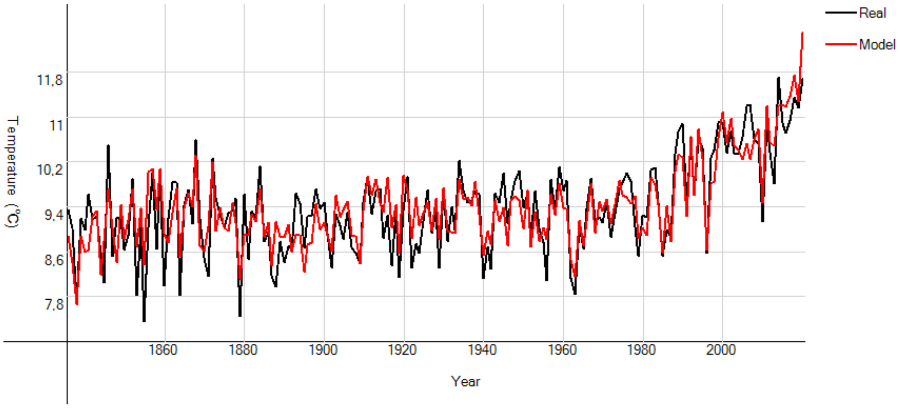

(a) Comparison between the real mean annual temperature and the estimates of the WP model

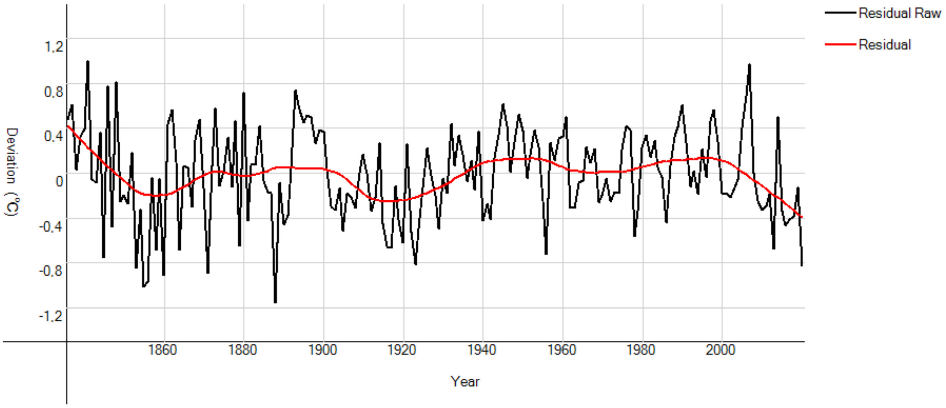

(b) The residuals

FIGURE 6 Results of the WP model. Here we use as explanatory variables the 96 weather patterns, together with the solar radiation, cloud coverage, and wind speed on the ground [Colour figure can be viewed at wileyonlinelibrary.com]

on the diagonal; for example, the variance of the TSI can be found as element (1, 1). If we denote this value by c, then we know that the standard deviation s_{TSI} of the TSI can be calculated as

$$s_{TSI} = \sqrt{c} \cdot \frac{S}{111}.$$

We can use this because the factor for the TSI follows a t-distribution with 111 degrees of freedom (see Walpole and Myers, 1993). The mean is the value we calculated above (so approximately 0.58) and we have just calculated the standard deviation. Using this, we can calculate a 95% confidence interval for the TSI. For the other factors we do the same. We can see that the TSI and AMO are significant, but the CO_2 is not. Figure 7 shows the total model, so the TSI, the AMO, the CO_2 and the influence of the weather patterns. This total model reaches even $R^2 = 0.85$. Also, there do not seem to be any systematic other signals in the residual. The residual is depicted using a Loess curve with span 0.3.

Remark that we could have included the TSI, AMO, and the CO_2 in our initial, daily linear regression model. We have chosen to explain the residuals as described above, since we do not have reliable data for the solar radiation, cloudiness, and wind speed for the period before 1960, which we need for the linear regression model.

We have also made a graph of the influences of the circulation, the TSI, the AMO, and the CO_2 on the temperature in the model above (see Figure 8). It clearly shows that the circulation is the dominant factor and that the TSI and the AMO are capable of producing small changes on a larger scale, whereas CO_2 seems to have no direct effect.

Remark that in this regression model we use CO_2 as an explanatory variable for the set of residuals. Hence, one could argue that the role of the CO_2 has been taken over by the WPs. Therefore, we have applied another regression model in which we have fixed the factor for the CO_2 according to the value widely assumed in climate models, which corresponds to an increase in temperature of 3° for each doubling of CO_2. We describe this model at the end of section 6.

It is unexpected that the factor of CO_2 is so low: in most studies, CO_2 has much more effect. Van Oldenborgh and Van Ulden (2003), for example, state that of the 1° of warming in the 20th century approximately 0.8 can be attributed to the general increase in temperature, which is usually used as a proxy for CO_2, and 0.2 to an

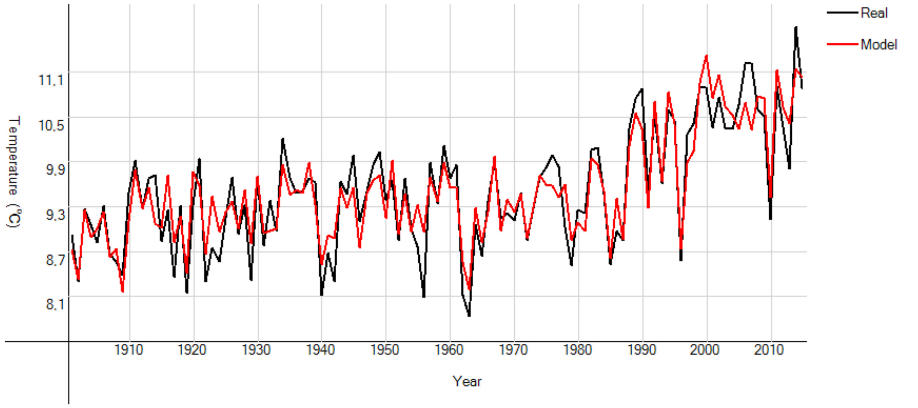

(a) The real data compared to the estimates of the complete model

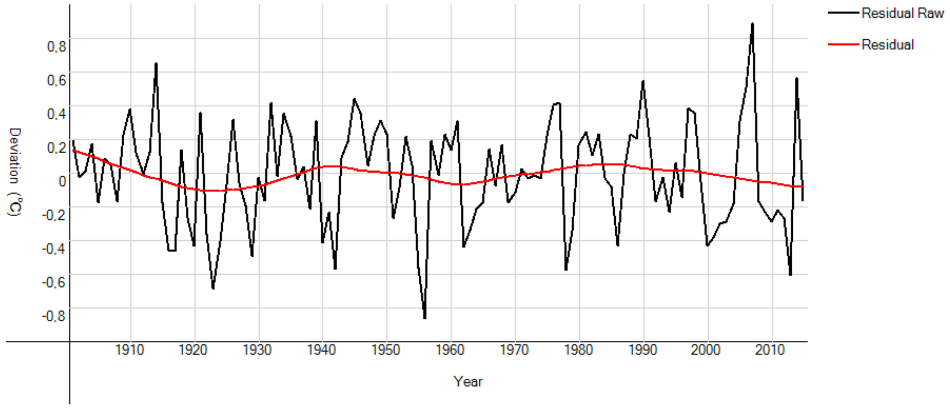

(b) The residuals for the complete model

FIGURE 7 Results of the complete model. Here we also use the AMO, TSI, and CO_2 as explanatory variables [Colour figure can be viewed at wileyonlinelibrary.com]

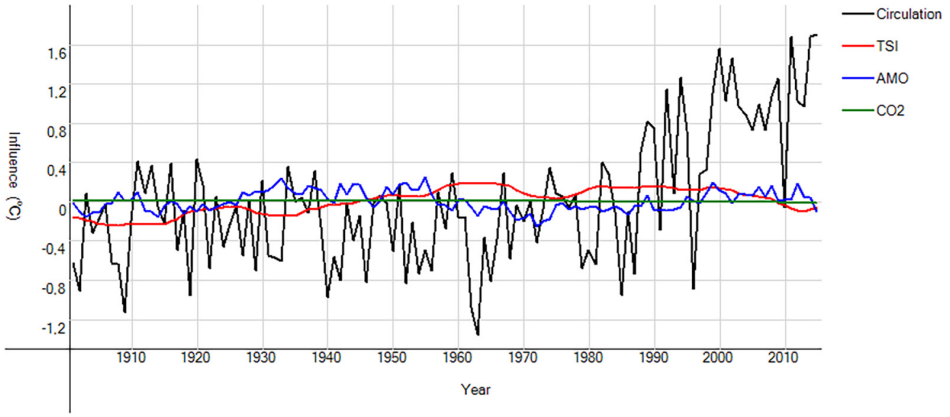

FIGURE 8 The influence of each factor on the temperature [Colour figure can be viewed at wileyonlinelibrary.com]

increase in warmer wind directions. Therefore, we have done some extra calculations to check our model, which we describe in section 6.

6 | CHECKING THE CORRECTNESS OF OUR MODEL

First of all, we checked the "jump": in 1988 the temperature suddenly jumped to a higher level. This jump is largest in January, February, and March, and it may have been caused by a clear change in atmospheric circulation. If so, it should be reproduced accurately in our model. In Figure 9 we compare the periods 1961–1987 to 1988–2015. In the left part, we show the average temperature for January 1 to March 31. In the right part, we show the difference between the average real temperature January–March and the average estimated temperature January–March.

The real temperature is approximately 1.8°C higher in 1988–2015 than in 1961–1987, whereas the temperature minus the estimate is approximately 0.03°C higher.

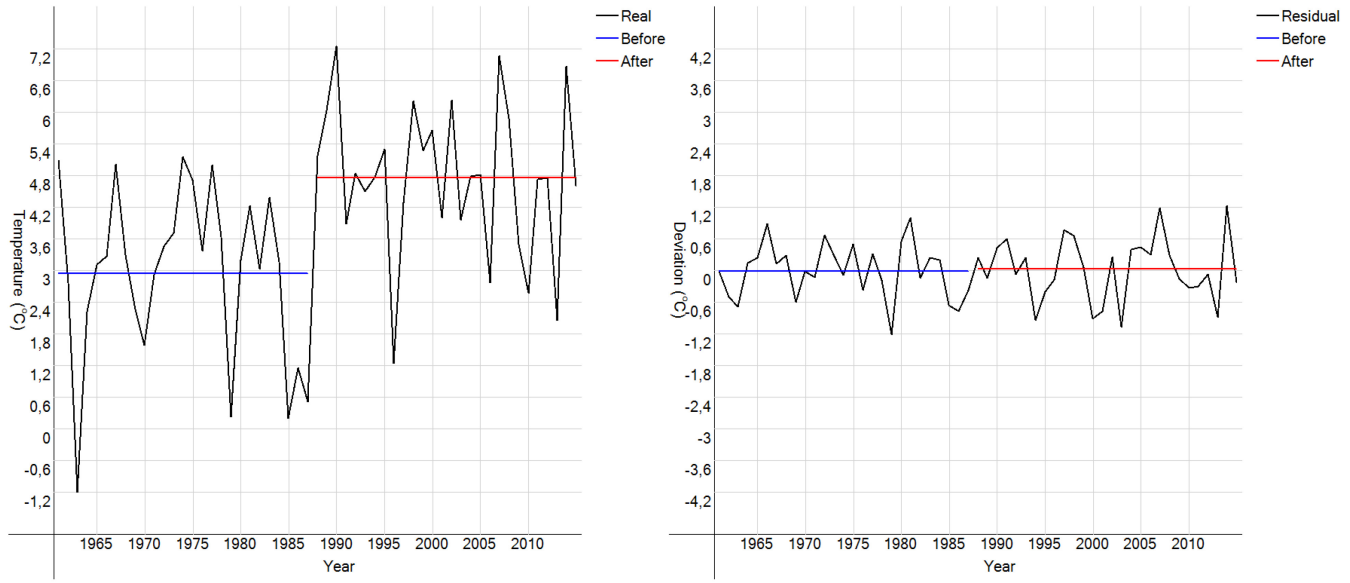

(a) The real temperature (b) The residuals of the model

FIGURE 9 The jump in the January to March temperature from 1987 to 1988 [Colour figure can be viewed at wileyonlinelibrary.com]

Both graphs have the same scale so it can also easily be seen that the fluctuations are much smaller for the residuals. Furthermore, the residuals just behave like noise around 0. This warrants the conclusion that our model explains this jump correctly. Moreover, if the factor for CO_2 in our model would be too low and the factor for the circulation too high, then the residual should have dropped in 1988 and gradually increased since then, as the amount of CO_2 rises steadily.

Second, we investigate the warming of the source regions. In our basic model we only use as explanatory variables the 96 weather patterns, together with the solar radiation, clouds, and the wind speed. One could argue that we do not take the warming of the source regions into account. Thereto, we have conducted four experiments, 2 with regard to CO_2 and 2 with regard to the average world temperature to correct for the warming of the source regions. Since CO_2 is assumed to be the driver behind the warming, we use CO_2 in our first two experiments. In the next two experiments we use the world average temperature instead. In the first experiment we have added CO_2 as the 100th explanatory variable in the regression in section 5 explaining the anomaly of the air temperature. We have further added CO_2 as a third explanatory variable in the model in which we estimate the influence of the sea. Next, we have subtracted the total estimated influence (including the sea) of the weather patterns, solar radiation, clouds and wind speed, but not the contribution of CO_2. Next, we calculated the influence of CO_2, the AMO, and the TSI on the residuals from 1901 to 2015 in exactly the same way as before. The outcome of this experiment was rather surprising: adding CO_2 as an explanatory variable did not result in a smaller influence of the WPs, but in a tiny bit larger influence. If we calculate the influence of the TSI, AMO, and CO_2 in the same way as above from 1901 to 2015 on these anomalies, we find that the influence of CO_2 has decreased a bit to -0.06 ± 0.15. Hence, we conclude that adding CO_2 as an approximation for the warming of the source regions does not alter the results.

In the second experiment, we have done the same as above, but this time, we use the world average temperature from Hadcrut 5 (which can be downloaded from the Climate Explorer of the KNMI) as extra explanatory variable instead of CO_2. We do everything else the same as above to see whether this has any impact. Again, this does not change the outcome: if we calculate the influence of the TSI, AMO and CO_2 at the end, the factor of CO_2 becomes -0.05 ± 0.15 which is again a tiny bit smaller then our original value. Hence, we conclude that adding the world average temperature does not alter the results either.

In the third experiment, we have conducted a test in which we fix the factor for CO_2 beforehand at 0.75, and then apply the regression model. Note that this factor of 0.75 corresponds to an increase in temperature of approximately 3° for each doubling of CO_2; this is the value estimated in the IPCC report of 2014 (see https://www.ipcc.ch/site/assets/uploads/2018/02/SYR_AR5_FINAL_full.pdf). Thereto, we first apply a preprocessing step, in which we correct the temperature for the increase in CO_2 using this factor by subtracting it from the measured

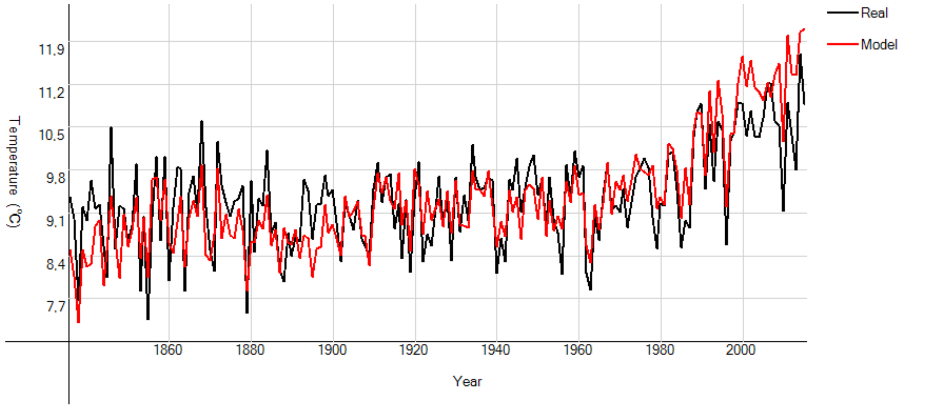

(a) The model with CO_2 (factor 0.75) compared to reality

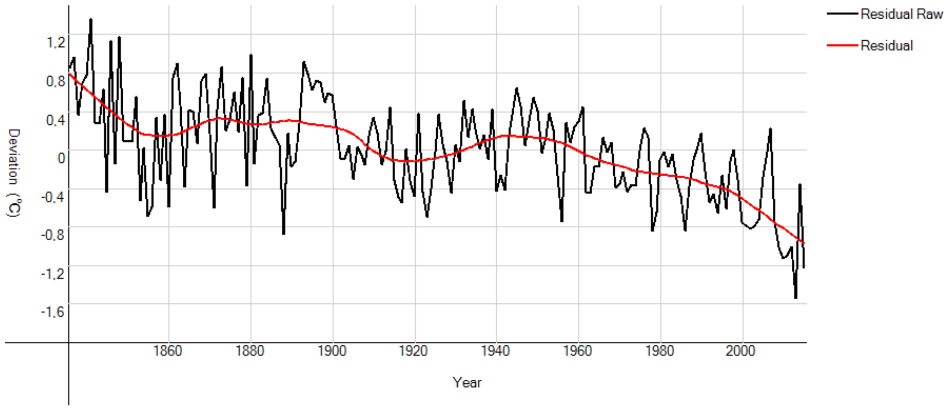

(b) The residuals for the model with CO_2

FIGURE 10 The model with fixed CO_2 influence (factor 0.75) [Colour figure can be viewed at wileyonlinelibrary.com]

temperature. Next, we estimate the influence of the weather patterns using a linear regression model in the same way as before, except that we have used the temperature corrected for CO_2 instead of the real data. We also again estimate the influence on the sea based upon this corrected temperature. In this way, we find the estimated temperature *without* CO_2. To get the estimated temperature *with* CO_2, we add the contribution of CO_2, which is the same amount we subtracted earlier. The resulting estimates with CO_2 are depicted in Figure 10a. In Figure 10b, we show the anomaly, that is, the real temperature minus the estimated temperature with CO_2, where we used a LOESS curve with span 0.2.

From Figure 10b it can clearly be seen that this model seems to overestimate the influence of CO_2: after a decrease from 1836 until something like 1850 the residual is reasonably constant at 0.3 until 1950, after which it decreases steadily until −1 in 2015. Even if we only use 1901–2015, the residual was around 1950 approximately 0.2 so it has decreased in the last 70 years with more than a degree. To see whether the model with the forced influence of CO_2 is correct, we have applied one final test. Hereto, we have first computed the real temperature minus the model without CO_2 for the years 1901–2015. We want to explain these residuals with the factors CO_2, AMO, and TSI; if the model with forced CO_2 influence is correct, we expect to find a factor of 0.75 for CO_2. Unfortunately, we get that the factor for CO_2 is 0.06 ± 0.15 which is significantly less than 0.75. This experiment clearly demonstrates that the WPs are the main contributing factor, and that in the regression model the daily differences are much more important than long-term deviations.

In our last experiment, we have done the same again, but this time, we subtracted the world average temperature with a factor 1. Next, we calculate the influence of the WPs once again on this corrected temperature as above. This does not alter the results: once again the influence of CO_2 is 0.06 ± 0.15 at the end. Since the graph of experiments 3 and 4 are very similar, we do not show the graph of experiment 4 here. We can thus conclude that the daily variations are much more important for the WPs than long-term deviations, which means that the WPs are not likely to overestimate their influence.

Given the results from above, we can clearly see that our method is not responsible for the possibly inaccurate low influence of CO_2: with our current data, this will pretty much always happen, even if we begin the model by assuming that CO_2 is the dominant factor for the warming in the Netherlands. The only manner in which

we can conclude that CO_2 is dominant is if we assume that that there are systematic mistakes in our data of the WPs such that we consistently overestimate warm WPs in the later years. We have therefore checked this possibility with another experiment. We have compared the WPs with the wind direction measured at the KNMI from 1961 to 2020 for each season; if there would be systematic mistakes in our classifications, then this comparison should show this. First, we binned the wind direction into eight categories just as we have done above. For each WP (so, e.g., N,G) we calculated how often the wind direction is in which category. We have simply done this by taking all the days with a certain weather pattern and measure the category of the wind direction. If for example there are only 5 days in winter over the entire period 1961–2020 with WP N,G, and the wind directions on these days are respectively N, N, NE, NW, N then we estimate in case of WP N,G that the probability of a N wind direction on the ground in De Bilt is 0.6; for NE and NW we then find probabilities of 0.2, and the other wind directions get probability 0. We have done this for all 25 WPs (so including the special type A). We now get per season 25 distributions for the wind direction on the ground in De Bilt. We assume that these 100 distributions are constant during the period 1961–2020. Then using these distributions, we estimate the total number of days with a certain wind direction per season per year. If for example the winter months of 1961 only have weather pattern N,G and the distribution of this weather pattern is 60% N, 20% NE, and 20% NW, then we estimate that in the winter months of 1961 exactly 54 days have wind from the north, exactly 18 days have wind from the northeast and exactly 18 days have wind from the northwest. We compare these estimates with the actual measurements at the KNMI by subtracting the actual measurements from the estimates. If the warm WPs would gradually have increased too much to take over the influence of CO_2, then we should see this: if for example S,G gradually increases too much, then in our estimate there should also be a gradual increase from wind from southern directions compared to the actual measurement. Table 5 shows the average of our estimates per season minus the measurements for the periods 1961–1990 and 1991–2020; the columns sometimes do not add up to zero because of rounding. It also shows the *t*-values of each shift and the *p*-values if significant. The column I shows the average from 1961 to 1990 and the column II shows the average from 1991 to 2020. If a value is positive, then this means that according to the weather patterns, there should have been more days with a certain wind direction in that season in that period. Hence, we can conclude for example from Table 5 (part a) that

TABLE 5 Comparison between the expected wind directions based on our weather patterns and the wind directions observed by the KNMI

(a) Winter				
Direction	**I**	**II**	***t*-value**	***p*-value**
NE	0.4	−0.4	−0.96	
E	0.4	−0.4	−0.86	
SE	−0.8	0.8	1.59	
S	0.3	−0.3	−0.48	
SW	0.7	−0.7	−1.06	
W	−0.3	0.3	0.68	
NW	−0.1	0.1	0.41	
N	−0.5	0.5	2.08	.04
(b) Spring				
Direction	**I**	**II**	***t*-value**	***p*-value**
NE	−0.8	0.8	1.5	
E	0.7	−0.7	−1.53	
SE	−0.6	0.6	1.63	
S	−0.7	0.7	1.49	
SW	0.7	−0.7	−1.29	
W	0	0	−0.06	
NW	0.3	−0.3	−0.56	
N	0.4	−0.4	−0.96	
(c) Summer				
Direction	**I**	**II**	***t*-value**	***p*-value**
NE	−1.3	1.3	2.29	.03
E	−0.1	0.1	0.3	
SE	0.3	−0.3	−1.08	
S	0	0	−0.04	
SW	1.7	−1.7	−2.74	.008
W	−0.1	0.1	0.2	
NW	−0.2	0.2	0.31	
N	−0.3	0.3	0.61	
(d) Autumn				
Direction	**I**	**II**	***t*-value**	***p*-value**
NE	−0.2	0.2	0.42	
E	0.5	−0.5	−1.22	
SE	0.5	−0.5	−1.23	
S	0.1	−0.1	−0.13	
SW	−0.4	0.4	0.56	
W	−0.8	0.8	1.56	
NW	0.9	−0.9	−2.46	.02
N	−0.6	0.6	1.67	

according to the weather patterns, there should have been 0.4 days more with wind from NE in 1961–1990 per winter than there actually were.

The shifts are relatively small (for example only two shifts are larger than 2 days) and they are relatively evenly divided between shifts to warmer and shifts to colder directions. There are only four types that are significant: N in winter, NE and SW in summer and NW in autumn. For N in winter, there have been more days in 1961–1990 than the WPs suggest and there have been fewer days in 1991–2020 than the WPs suggest. This means that the WPs with north should actually have decreased a day per winter, so the WPs underestimate the warming of the circulations for this type. For NE in summer, the WPs have increased too much which overestimates the warming influence. For SW in summer, however, the WPs have decreased too much, which underestimates the warming. Finally, for NW in autumn the WPs have decreased too much which overestimates the warming. To check if even these small changes have had any influence on the temperature, we have estimated their effect. For ease of computation, we attribute all differences to the WPs without a bend. For example in winter when NE was 0.4 too high and is now −0.4 too low in the model, we find that the model has 0.8 days NE,G too many in the period 1961–1990 compared to the period 1991–2020. We have multiplied this with the average effect of NE,G in winter (so this is largely the winter variable NE,G from the regression above plus a tiny part of the spring and autumn variable of NE,G from above) estimated in the linear regression model. We have summed up all these influences of every direction and every season. If we calculate this, we get that the estimates by the WPs are less than 0.01°C too warm in 1991–2020 compared to 1961–1990. This is of course completely negligible, and it suggests that the data of the WPs is also correct.

7 | CONCLUSIONS

In this paper, we have investigated the influence of the atmospheric circulation on the temperature in the Netherlands. Since these data were not available, we have first manually estimated for each day from 1836 until 2020 the atmospheric circulation on basis of the isobars in the weather maps from Wetterzentrale, which information we have stored in so-called weather patterns. Here we denoted the *origin* of the airflow instead of the direction of the final part of the trajectory of the airflow, and we showed that there often is a major difference between the origin of the airflow and the direction of the wind on the ground. Next, we have shown that the frequency of some of the weather patterns has changed significantly by comparing the periods 1961–1990 and 1991–2020, resulting in an increase of airflow coming from warmer directions. Finally, we have used the weather patterns to explain the daily temperature in the Netherlands; hereto, we used a model based on linear regression. When we extended the model with a factor representing the sea, and with factors for the TSI, AMO, and CO_2, then we find an R^2 value of 0.85. Interestingly enough, CO_2 does not seem to play a role. To arm ourselves against the possibility that wrongly the influence of CO_2 was attributed to some other, dependent variable, we have adjusted the model by fixing the coefficient of CO_2 to a value corresponding to a warming of 3° for a doubling of CO_2. This did not change the influence of the WPs much, while the influence of CO_2 remained insignificant. Similarly, we have armed ourselves against the influence of the warming up of the source regions over time. Hereto, we have simply corrected the measured temperatures by subtracting the average world temperature and then repeating the experiments above. On basis of both experiments, we can conclude that our method has not incorrectly underestimated the influence of CO_2. We have also checked whether the WPs are perhaps incorrectly favouring warm wind directions in the more recent years by comparing their frequencies to the frequency of the wind on the ground. Our experiments did not show such systematic mistakes, and therefore, we cannot but conclude that indeed the air circulation is the main force behind the temperature increase in the Netherlands. In this way, we follow the conclusions by Lamb and Johnsson (1959), who researched the change in climate that has resulted in a strong warming of the Northern Hemisphere since 1800. They considered a large number of possible causes, one of which is a change in circulation patterns. For their investigation they considered the monthly mean pressure maps and translated these into mean circulation patterns. They concluded that this warming is strongly related to an increased intensity of the circulation.

We hope that our research will be repeated in other regions. There are quite some further open questions left that are worth being investigated. The most important one is of course: what mechanism is responsible for the change in atmospheric circulation? Is CO_2 responsible for this change? Or is it because of natural causes? Recent research suggests that in the Mid-Holocene similar wind conditions applied as currently (Mauri *et al.*, 2014). A second interesting line of research is to find out why CO_2 does not seem to contribute to the rise in temperature; is there a negative feedback that compensates it?

ACKNOWLEDGEMENT

We want to thank Prof. Dr. Marie-Colette van Lieshout for her help in verifying our statistical models. Furthermore,

we have made the data, in which we describe the classification in Weather Patterns together with the estimates of the windspeed, available at the website https://webspace.science.uu.nl/~hooge109/WP/Data.html.

ORCID

Han Hoogeveen https://orcid.org/0000-0001-8544-8848

REFERENCES

Bartoszek, K. and Matuszko, D. (2021) The influence of atmospheric circulation over Central Europe on the long-term variability of sunshine duration and air temperature in Poland. *Atmospheric Research*, 251, 105427. https://doi.org/10.1016/j.atmosres.2020.105427.

Bergeron, T. (1928) Über die dreidimensional veknüpfende Wetteranalyse. Erster Teil. Prinzipelle Einführung in das Problem der Luftmassen- und Frontenbildung. *Geofysics Publication*, 5, 1–111.

Gerstengarbe, F.W. and Werner, P.C. (2005) *Katalog der GrossWetterLagen Europas KATALOG (1881–2004)*. Potsdam: Potsdam-Institut für Klimafolgenforschung (in German).

Huth, R. (1996) An intercomparison of computer-assisted circulation classification methods. *Internationational Journal of Climatology*, 16, 893–922. https://doi.org/10.1002/(SICI)1097-0088(199608)16:8<893::AID-JOC51>3.0.CO;2-Q.

Huth, R., Beck, C., Philipp, A., Demuzere, M., Ustrnul, Z., Cahynová, M., Kyselý, J. and Tveito, O.E. (2008) Classifications of atmospheric circulation patterns. Recent advances and applications. *Trends and Directions in Climate Research*, 1146, 105–152. https://doi.org/10.1196/annals.1446.019.

Isaksen, K., Nordli, Ø., Førland, E.J., Łupikasza, E.E., Eastwood, S. and Niedźwiedź, T. (2016) Recent warming on Spitsbergen: influence of atmospheric circulation and sea ice cover. *Journal of Geophysical Research: Atmospheres*, 121, 11913–11931. https://doi.org/10.1002/2016JD025606.

James, P.M. (2007) An objective classification method for Hess and Brezowsky Grosswetterlagen over Europe. *Theoretical and Applied Climatology*, 88, 17–42. https://doi.org/10.1007/s00704-006-0239-3.

Lamb, H.H. (1972) British Isles weather types and a register of the daily sequence of circulation patterns, 1861–1971. *Geophysical Memoirs*, 116, 1–85.

Lamb, H.H. and Johnsson, A.I. (1959) Climatic variation and observed changes in the general circulation. Parts I and II. *Geografiska Annaler*, 41, 94–134.

Leśniok, M., Małarzewski, Ł. and Niedźwiedź, T. (2010) Classification of circulation types for southern Poland with an application to air pollution concentration in Upper Silesia. *Phsyics and Chemistry of the Earth, Parts A/B/C*, 35, 516–522. https://doi.org/10.1016/j.pce.2009.11.006.

Mauri, A., Davis, B.A.S., Collins, P.M. and Kaplan, J.O. (2014) The influence of atmospheric circulation on the mid-Holocene climate of Europe: a data-model comparison. *Climate of the Past*, 10, 1925–1938. https://doi.org/10.5194/cp-10-1925-2014.

Niedźwiedź, T. (2006) Typology of circulation for Poland and methods of circulations the regional circulation indices. *Annales Universitatis Mariae Curie-Sklodowska Lublin-Polonia, Section B*, 38, 326–335.

Przybylak, R. and Maszewski, R. (2009) Influence of atmospheric circulation on air temperature and precipitation in the Bydgoszcz-Toruń region in the period from 1921 to 2000. *Bulletin of Geography*, 1, 18–37.

Van Oldenborgh, G.J., Drijfhout, S., Van Ulden, A., Haarsma, R., Sterl, A., Severijns, C., Hazeleger, W. and Dijkstra, H. (2009) Western Europe is warming much faster than expected. *Climate of the Past*, 5, 1–12. https://doi.org/10.5194/cp-5-1-2009.

Van Oldenborgh, G.J. and Van Ulden, A. (2003) On the relationship between global warming, local warming in the Netherlands and changes in circulation in the 20th century. *International Journal of Climatology*, 23, 1711–1724. https://doi.org/10.1002/joc.966.

Walpole, R.E. and Myers, R.H. (1993) *Probability and Statistics for Engineers and Scientists*, 5th edition. New York, NY: Macmillan.

How to cite this article: Hoogeveen, J., & Hoogeveen, H. (2023). Winds are changing: An explanation for the warming of the Netherlands. *International Journal of Climatology*, *43*(1), 354–371. https://doi.org/10.1002/joc.7763